

Global Density Analysis for an Off-Lattice Cellular Automata Model

Michael A. Yereniuk ^{*} Sarah D. Olson [†]

June 6, 2022

KEYWORDS: Cellular Automata, Interaction Neighborhood, Global Recurrence Rule, Stability Analysis

Abstract

Agent-based (AB) or Cellular Automata (CA) models are rule based and are a relatively simple discrete method that can be used to simulate complex interactions of many agents or cells. The relative ease of implementing the computational model is often counterbalanced by the difficulty of performing rigorous analysis to determine emergent behaviors. In addition, without precise definitions of cell interactions, calculating existence of fixed points and their stability is not tractable from an analytical perspective and can become computationally expensive, involving potentially thousands of simulations. Through developing a precise definition of an off-lattice CA or AB model with a specified interaction neighborhood, we develop a general method to determine a Global Recurrence Rule (GRR). This allows estimates of the state densities in time, which can be easily calculated for a range of parameters in the model. The utility of this framework is tested on an Epidemiological Cellular Automata (E-CA) model where agents or cells correspond to people that are in the susceptible, infected, or recovered states. The interaction neighborhoods of cells are determined in a mathematical formulation that allows the GRR to accurately predict the long term behavior and steady states. The modeling framework outlined will be generally applicable to many areas and can be easily extended.

^{*}Department of Mathematical Sciences, Worcester Polytechnic Institute, Worcester, MA (mayereniuk@wpi.edu)

[†]Department of Mathematical Sciences, Worcester Polytechnic Institute, Worcester, MA (sdolson@wpi.edu)

1 Introduction

When the goal is to understand a complex system of interacting agents or cells that are decision makers, there are several different modeling frameworks from which to choose. Often, if the focus is on understanding and capturing each of the individual interactions and movement, a Lagrangian framework such as a Cellular Automaton (CA) or Agent Based (AB) model is used [14, 15, 18, 26]. When we are interested in global dynamics, or are more interested in how the field is evolving, Eulerian equation based approaches are utilized, e.g. difference equations or systems of differential equations. For each of these frameworks, there are different pros and cons with respect to the ability to formalize and analyze a model, as well as the ease with which one can simulate the model [24]. There are many challenges, which can arise due to noise, nonlinearities, and other spatial or temporal variations in the system [30].

In CA or AB models, the cells or agents are each individually assessing their surrounding environment, potentially moving or changing state at each time increment based on a given set of rules [3]. The state dependent rules could be deterministic or stochastic, and are quite often a nonlinear function based on information (e.g. other agents, states, or other environmental factors) in a locally defined cellular interaction neighborhood [11]. The movement can be on-lattice with discretely defined locations that are assigned a given probability. For example, if a lattice is a regular, 2-dimensional grid, the on-lattice movement of a given agent could be either horizontal or vertical movement to an adjacent lattice node at each time increment [13, 31]. Movement can also be off-lattice, where a cell can move a given step size in a particular direction, where the location does not have to lie on a predefined grid of locations. Often, questions of interest concern the emergent behavior of a large number of interacting agents, which can be hard to capture at the continuous scale [15]. We note that since this modeling framework is quite general, the cell or agent could represent any feature of interest in a given system [28], which is why these types of models are frequently used for social, biological, financial, and military applications [1, 3, 7, 9, 12, 13, 16, 25, 31]. In terms of biological applications at the cellular level, AB or CA models have been used to investigate tumor growth where the agents are the individual cells that make up the tumor [16], sperm cell motility where the sperm are the individual agents [4, 5], and signaling pathways within and on the membrane of cells where agents are molecules and receptors [3].

It is well known that as the number of agents in a system increases, this may cause simulations investigating long term dynamics to become intractable [15]. Additionally, there is generally a desire to understand how model outcomes change with respect to varying parameter values [8], which again would necessitate possibly thousands of simulations. As described previously, there is not a universal or agreed upon standard to specify these models and in many cases, the mathematical description of the rules are also not specified [14].

The focus of this current work is an introduction of a theoretical formalism and subsequent analysis of an off-lattice CA or AB model where agents or cells exhibit stochastic behavior when moving and changing states. Specifically, the necessary notation for the CA model is outlined in Section 2.1, which is similar to previous work [11, 14]. Different from other approaches, our setup relies heavily on a precise definition of the interaction neighborhoods of agents, which we view as a region where a cell potentially exerts state changes to other cells. In Section 2.2, we detail how to derive a Global Recurrence Rule (GRR) to determine the expected value for the number of agents in each state when assuming that a cell’s state and movement are solely determined by the cell’s current status. To show the applicability of this formalism, in Section 3, we illustrate how a GRR can be derived for an epidemiological-CA (E-CA) model that captures the spread of an infection such as influenza. The long term behavior and steady state solutions obtained for the infected, recovered, and susceptible states using our GRR have good agreement with simulations and we are able to prove stability of fixed points. In addition, we illustrate with the E-CA how to use additional information about the dynamics to develop a more refined local approximation of the neighborhoods, with reduced error. In Section 4, we compare the different models and emphasize which assumptions need to be satisfied in order for the GRR to be a valid approximation for the E-CA model.

2 Initial Definitions

2.1 CA Notation

A Cellular Automaton (CA) is an agent-based model, where we track the state and location of individual cells. We first need to create a precise definition of the properties of the cells and their interactions in order to determine

the correct governing equations and hence be able to mathematically analyze the model. We define a bounded region of interest Ω in which we track the cells. We suppose that we have a finite collection, \mathcal{X} , of N cells indexed by $1, \dots, k-1, k, k+1, \dots, N$. At every time $t \geq 0$, each cell k is assigned one and only one state s_k^t and location \mathbf{x}_k^t . We define the set containing all possible cellular states as the state space $\Sigma = \{\mathcal{U}_1, \mathcal{U}_2, \dots\}$. That is, for each cell k and time t , we necessitate that $s_k^t = \mathcal{U}_i$ for exactly one state $\mathcal{U}_i \in \Sigma$.

The domain, Ω , may be either a discrete set of nodes connected by edges or a continuous, bounded subset of \mathbb{R}^M for some $M \in \mathbb{N}$. If Ω is discrete, we say these cells exist on-lattice. Otherwise, if Ω is continuous, we say these cells exist off-lattice. In either case, the cells can either be stationary or move. The cell movement can be deterministic, but usually it is some type of random walk, governed by a model specific probability distribution [7, 10, 25]. It is important to note that the scalings and distributions may be spatially, temporally, or state dependent.

A CA is a model locally defined by the pair $\mathcal{A} = (f, \mathcal{N})$, where we denote the collection of neighborhoods for each cell as $\mathcal{N} = \{\mathcal{N}^1, \mathcal{N}^2, \dots, \mathcal{N}^N\}$ and f is a local transition rule, which defines how cells change states [11]. If the model specifies that each neighborhood is temporally or state dependent, we define \mathcal{N}_t^j as the neighborhood of cell j in state s_t^j at iteration t . We emphasize that the neighborhood \mathcal{N}_t^j is the region of influence in which cell j may exert state changes to other cells¹. The local transition rule is a function $f : \mathcal{X} \rightarrow \Sigma$. Since each cell belongs to one and only one state, the local transition rule f is well-defined. The function assignment $s_{t+1}^k = f(s_t^k)$ depends conditionally on the neighborhoods in which \mathbf{x}_t^k is contained.

Define $B_t^{\mathcal{V}, \mathcal{U}}$ as the $\mathcal{V} \rightarrow \mathcal{U}$ transition region² at time t . That is, $B_t^{\mathcal{V}, \mathcal{U}}$ is the region such that if, at time t , there is some cell k such that $s_t^k = \mathcal{V}$ and $\mathbf{x}_t^k \in B_t^{\mathcal{V}, \mathcal{U}}$, then cell k can transition to state \mathcal{U} at time $t + 1$. In terms of our neighborhoods of influence, we can formally define the transition region as follows.

Definition 1. *The $\mathcal{V} \rightarrow \mathcal{U}$ transition region at time t is $B_t^{\mathcal{V}, \mathcal{U}} = \bigcup_{j \in \mathcal{C}} \mathcal{N}^j$, with*

¹ Traditional CA definitions define the neighborhood \mathcal{N}_t^j as the region in which other cells exert state changes to cell j . However, we assert the opposite — \mathcal{N}_t^j is the region in which cell j exerts state changes to other cells. This perspective allows us greater freedom to model more realistic state and property-dependent neighborhoods.

²In general, cells in states other than \mathcal{U} can cause cells to transition to state \mathcal{U} .

$\mathcal{C} = \left\{ j \mid \exists k \text{ such that } s_t^k = \mathcal{V} \text{ and } \mathbf{x}_t^k \in \mathcal{N}_t^j \Rightarrow \mathbb{P}(f(s_t^k) = \mathcal{U}) > 0 \right\}$ the indexing set.

Our explicit definition of the transition region $B_t^{\mathcal{V}, \mathcal{U}}$ for each $\mathcal{V}, \mathcal{U} \in \Sigma$ will allow us to clearly define $f(s_t^k)$.

We are interested in finding a Global Recurrence Rule (GRR), which calculates the expected density of cells in a state at each iteration throughout Ω . Let $\mathcal{U} \in \Sigma$, with U_t denoting the number of cells in state \mathcal{U} at iteration t (that is, $U_t = |\{k : s_t^k = \mathcal{U}\}|$). We denote $W(\mathcal{V} \rightarrow \mathcal{U})$ to be the transition probability that a cell in state \mathcal{V} at iteration t transitions to state \mathcal{U} at time $t + 1$. We summarize our CA notation in Glossary 1.

- \mathcal{X} : the collection of cells (indexed as $1, \dots, k - 1, k, k + 1, \dots, N$)
- Σ : state space
- s_t^k : the state of cell k at time t
- Ω : the bounded region of interest
- \mathbf{x}_t^k : the location of cell k at time t
- \mathcal{N}_t^k : neighborhood of cell k at time t
- $f : \mathcal{X} \rightarrow \Sigma$: the transition rule that assigns each cell at time t to a unique state at time $t + 1$
- U_t : the number of cells in state \mathcal{U} at time t
- $B_t^{\mathcal{V}, \mathcal{U}}$: the $\mathcal{V} \rightarrow \mathcal{U}$ transition region
- $W(\mathcal{V} \rightarrow \mathcal{U})$: the probability a cell in state \mathcal{V} transitions to state \mathcal{U}

Glossary 1: Cellular Automata Terms

2.2 Global Recurrence Rule

We now have the necessary notation to derive the expected density of a state at any given time. The state of a cell k at $t + 1$ only depends on its state (s_t^k)

and location (\mathbf{x}_t^k) at time t , making this a Markovian process [6]. Hence, the probability that cell k is in state \mathcal{U} at time $t + 1$ given that the cell was in state \mathcal{V} at time t reduces to

$$\mathbb{P}\left(s_{t+1}^k = \mathcal{U} \mid s_t^k = \mathcal{V}\right) = \mathbb{P}\left(\mathbf{x}_t^k \in B_t^{\mathcal{V}, \mathcal{U}}\right) W(\mathcal{V} \rightarrow \mathcal{U}), \quad (1)$$

the product of the probability that cell k is located in a $\mathcal{V} \rightarrow \mathcal{U}$ transition region with the probability that cell k transitions from state \mathcal{V} to state \mathcal{U} . We can then find $\mathbb{E}(U_{t+1})$, the expected number of cells in state \mathcal{U} at iteration $t + 1$, by

$$\mathbb{E}(U_{t+1}) = \mathbb{E}\left(|\{k : s_{t+1}^k = \mathcal{U}\}|\right) \quad (2)$$

$$= \sum_{k=1}^N \mathbb{P}\left(s_{t+1}^k = \mathcal{U}\right) \quad (3)$$

$$= \sum_{\mathcal{V} \in \Sigma} \sum_{\{k: s_t^k = \mathcal{V}\}} \mathbb{P}\left(s_{t+1}^k = \mathcal{U} \mid s_t^k = \mathcal{V}\right) \quad (4)$$

$$= \sum_{\mathcal{V} \in \Sigma} \sum_{\{k: s_t^k = \mathcal{V}\}} \mathbb{P}\left(\mathbf{x}_t^k \in B_t^{\mathcal{V}, \mathcal{U}}\right) W(\mathcal{V} \rightarrow \mathcal{U}). \quad (5)$$

Note that equality between (3) and (4) is due to the fact that we can partition the collection of cells \mathcal{X} by the distinct states in Σ . This leads us to the definition of the Global Recurrence Rule (GRR).

Definition 2. Let $\mathcal{U}, \mathcal{V} \in \Sigma$, $U_t = |\{k : s_t^k = \mathcal{U}\}|$, and $B_t^{\mathcal{V}, \mathcal{U}}$ be the $\mathcal{V} \rightarrow \mathcal{U}$ transition region at time t . We define the Global Recurrence Rule (GRR) as

$$\mathbb{E}(U_{t+1}) = \sum_{\mathcal{V} \in \Sigma} \sum_{\{k: s_t^k = \mathcal{V}\}} \mathbb{P}\left(\mathbf{x}_t^k \in B_t^{\mathcal{V}, \mathcal{U}}\right) W(\mathcal{V} \rightarrow \mathcal{U}).$$

Thus, to find expected values of states analytically, one just needs a framework to denote and calculate both the probability of being in a transition region and the probability that a cell in the transition neighborhood will transition to a particular state.

3 Application to Disease Dynamics

3.1 Phenomenological Perspective

Disease dynamics provides an interesting case study to determine the validity of the GRR. Assume there are infected individuals in a population. For simplicity, we can divide the remaining population into two classes, those who are susceptible to infection and those who were infected but cannot currently infect other individuals. We denote these classes “susceptible” and “recovered,” respectively. Further, suppose that after a finite time the recovered can become susceptible to infection again. That is, an individual in the recovered state is temporarily conferred immunity before returning to the susceptible state. This is often referred to as an SIR Epidemiological model, where simulations and analysis have been an active research area for many years [29], especially with respect to endemic equilibrium sizes [21, 23] and infectivity wave speed [22]. The modeling framework for SIR Epidemiological studies have been based on differential equations, networks, and agent based models; each approach has provided some successes. Challenges still exist to capture the relevant dynamics and to make time sensitive and accurate predictions with regards to disease outbreaks [2, 20, 21, 22, 23, 29, 30].

In terms of the CA framework presented in Section 2, it is relatively straightforward to implement an epidemiological CA (E-CA) model. There are only 3 states: \mathcal{S} (susceptible), \mathcal{I} (infected), and \mathcal{R} (recovered). In addition, the only neighborhoods of interest are those belonging to the infected cells since they will influence the state change of susceptible cells in their region of influence.

3.2 Epidemiological Cellular Automata

To simplify, we let the continuous domain, Ω , of the E-CA be the unit square. The cells remain in the infected and recovered states for T_i and T_R iterations, respectively. Thus, our state space for the E-CA is $\Sigma = \{\mathcal{S}, \mathcal{I}_1, \mathcal{I}_2, \dots, \mathcal{I}_{T_I}, \mathcal{R}_1, \mathcal{R}_2, \dots, \mathcal{R}_{T_R}\}$. This dynamic is also referred to as an $SI^{T_I}R^{T_R}$ model [21].

We initialize N cells in Ω such that $N - 1$ cells are in state \mathcal{S} ($S_0 = N - 1$) and one cell is in state \mathcal{I}_1 ($I_0 = 1$), where $S_t = |\{k : s_t^k = \mathcal{S}\}|$ and $I_t = \cup_{j=1}^{T_I} |\{k : s_t^k = \mathcal{I}_j\}|$ for each time t . We index the initially infected cell as $k = 1$, and initialize its location in the center of the region Ω . The susceptible

cells are randomly initialized following a uniform random distribution (i.e. $\mathbf{x}_0^k \sim \text{Uniform}(\Omega)$ for $k = 2, 3, \dots, N$).

Each cell³ moves by a uniform random walk inside Ω . If $\mathbf{x}_t^k = (x, y)$, then $\mathbf{x}_{t+1}^k = (x + \Delta r \cos \theta, y + \Delta r \sin \theta)$, where $\theta \sim \text{Uniform}[0, 2\pi)$ and $\Delta r \ll 1$ is the constant radial spatial step. Reflective boundary conditions are enforced along $\partial\Omega$. That is, if a cell hits the boundary (or is about to move outside of Ω), it is shifted a distance Δr into Ω along the direction normal to the boundary.

For our E-CA, we assume that the infectivity neighborhood of any infected cell k is radially symmetric with radius ρ_0 . That is, $\mathcal{N}_t^k = \{\mathbf{y} \in \Omega : \|\mathbf{y} - \mathbf{x}_t^k\|_2 \leq \rho_0\}$, the collection of all points of a distance less than ρ_0 away from cell k , is the area in which susceptible cells can become infected by cell k .

Now consider any cell k such that $s_t^k = \mathcal{S}$. In order for cell k to become infected, we require \mathbf{x}_t^k to be in an infected neighborhood, regardless of the iteration of infectivity. We define the $\mathcal{S} \rightarrow \mathcal{I}_1$ transition region as $B_t^{\mathcal{S}, \mathcal{I}_1} = \bigcup_{\{k: s_t^k = \mathcal{I}_j, \exists j\}} \mathcal{N}_t^k$. Recall that the \mathcal{S} to \mathcal{I}_1 transition region is the region in which a cell in state \mathcal{S} can transition to state \mathcal{I}_1 . The susceptible cell has the potential to become infected when in at least one neighborhood of an infected cell at any state of the infection (for $j = 1, \dots, T_I$). In this simple E-CA model, the number of infectivity neighborhoods in which cell k is located does not affect the probability of cell k being infected. The susceptible cells located inside $B_t^{\mathcal{S}, \mathcal{I}_1}$ become infected with probability $1 - \kappa$, where $\kappa \in [0, 1]$ is the contact tolerance. For simplification, we will assume that ρ_0 and κ are scalar constants⁴ and the transition rules between states are given below.

Definition 3. *The following local transition rule $f : \mathcal{X} \rightarrow \Sigma$, such that*

³ For simplicity, every cell in this model moves according to the same rules. However, one could produce a model where each state moves differently. For example, the infected cells could move at a much smaller spatial step than the susceptible or recovered cells.

⁴ Our E-CA is a toy example to demonstrate the efficacy of the GRR. For simplification, ρ_0 and κ are constants. In practice, ρ_0 and κ should be random variables drawn from specific probability distributions, such as the models found in [20].

$s_{t+1}^k = f(s_t^k)$ are given as follows:

$$\text{If } s_t^k = \mathcal{S} : \quad f(s_t^k) = \begin{cases} \mathcal{I}_1 & : \text{ if } \mathbf{x}_t^k \in B_t^{\mathcal{S}, \mathcal{I}_1} \text{ and } \kappa > X, \\ & \text{where } X \sim \text{Uniform}[0, 1] \\ \mathcal{S} & : \text{ otherwise} \end{cases} \quad (6)$$

$$\text{If } s_t^k = \mathcal{I}_j, \exists j = 1, 2, \dots, T_I : \quad f(s_t^k) = \begin{cases} \mathcal{I}_{j+1} & : \text{ if } 1 \leq j < T_I \\ \mathcal{R} & : \text{ if } j = T_I \end{cases} \quad (7)$$

$$\text{If } s_t^k = \mathcal{R}_m, \exists m = 1, 2, \dots, T_R : \quad f(s_t^k) = \begin{cases} \mathcal{R}_{m+1} & : \text{ if } 1 \leq m < T_R \\ \mathcal{S} & : \text{ if } m = T_R \end{cases}. \quad (8)$$

Figure 1 illustrates the off-lattice CA simulation as outlined above using $N = 10000$ cells, where the susceptible, infected, and recovered cells are colored as black, red, and green, respectively. We implemented each iteration by first determining the region of infectivity from a constant infectivity radius of $\rho_0 = 0.04$. We then updated the cell states according to the above transition rules (6)–(8) with contact tolerance $\kappa = 0.95$. This “high” contact tolerance relates to a “low” probability of a susceptible cell becoming infected. Moreover, the time spent in the infective state and the time spent in the recovered state are $T_I = T_R = 30$. Finally, we update the cell location by performing unbiased random walks with $\Delta r = 0.001$.

3.3 Globally Homogeneous GRR

To reduce the number of equations, we can assume a Markovian (time-independent) process. We simplify the number of states by defining $\mathcal{I} = \bigcup_{i=1}^{T_I} \mathcal{I}_i$ as the infected state, which is independent of the amount of time spent in the infected state. Similarly, we define $\mathcal{R} = \bigcup_{i=1}^{T_R} \mathcal{R}_i$, the total number of recovered cells, regardless of the amount of time spent in the recovered state. We are primarily interested in calculating the expected total number of infected and recovered cells at each particular iteration t , not the particular stage of the infection or recovery.

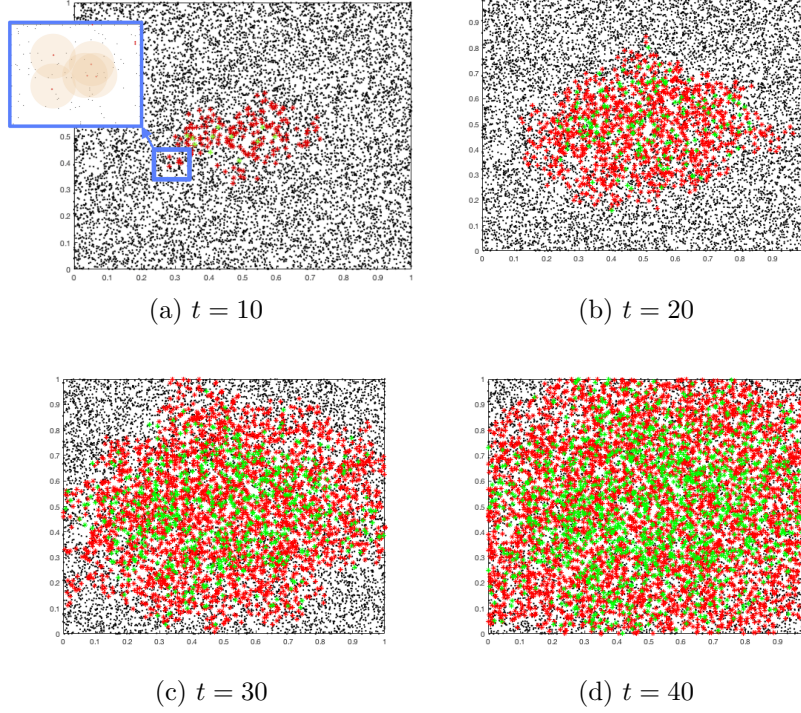


Figure 1: Simulation of 10000 cells at various time steps with a single cell infected initially, which is located at $(0.5, 0.5)$. The states are denoted as \blacksquare Susceptible, \blacksquare Infected, \blacksquare Recovered. The simulation parameters are defined as: contact tolerance - $\kappa = 0.95$, infectivity radius - $\rho_0 = 0.04$, infection time - $T_I = 30$, recovered time - $T_R = 30$, and spatial step - $\Delta r = 0.001$. As time increases, the epidemic spreads as a wave throughout the domain. The inset on (a) shows the radially symmetric neighborhoods of a few infected cells.

Adapting equation (5) to our E-CA model, we have the system

$$S_{t+1} = \sum_{\{k:s_t^k=\mathcal{S}\}} W(\mathcal{S} \rightarrow \mathcal{S}) + \sum_{\{k:s_t^k=\mathcal{R}\}} W(\mathcal{R} \rightarrow \mathcal{S}) \quad (9)$$

$$I_{t+1} = \sum_{\{k:s_t^k=\mathcal{S}\}} \mathbb{P}(\mathbf{x}_t^k \in B_t^{\mathcal{S}, \mathcal{I}}) W(\mathcal{S} \rightarrow \mathcal{I}) + \sum_{\{k:s_t^k=\mathcal{I}\}} W(\mathcal{I} \rightarrow \mathcal{I}) \quad (10)$$

$$R_{t+1} = \sum_{\{k:s_t^k=\mathcal{I}\}} W(\mathcal{I} \rightarrow \mathcal{R}) + \sum_{\{k:s_t^k=\mathcal{R}\}} W(\mathcal{R} \rightarrow \mathcal{R}) \quad (11)$$

The total number of cells is constant, so $S_t = N - (I_t + R_t)$. This allows the reduction of the above system to just two equations, namely (10) and (11). We will now determine the expressions for the probabilities.

We further simplify the derivation by ignoring the effect of the boundary on the infectivity neighborhood, which allows the assumption that the area of the region \mathcal{N}_t^k is independent of k and t . Let $\mu(\mathcal{N})$ denote the area of any neighborhood \mathcal{N}_t^k . Since our simulation is 2-dimensional, we then make the approximation⁵ that $\mu(\mathcal{N}) := \mu(\mathcal{N}_t^k) = \pi\rho_0^2$ for all k and t . It follows that the probability that the k th cell is located in the neighborhood of the j th cell is

$$\mathbb{P}(\mathbf{x}_t^k \in \mathcal{N}_t^j) = \frac{\mu(\mathcal{N})}{\mu(\Omega)}, \quad \forall j, \quad (12)$$

the ratio of the area of the infectivity neighborhood and the area of the region.

For any susceptible cell k to transition to state \mathcal{I} , it is sufficient that $\mathbf{x}_t^k \in B_t^{\mathcal{S},\mathcal{I}}$. If we assume that the transition probability $W(\mathcal{S} \rightarrow \mathcal{I})$ does not depend on the number of infectivity neighborhoods and that the infectivity neighborhoods are uniformly distributed within Ω , then by the multiplication rule of independent events,

$$\mathbb{P}(\mathbf{x}_t^k \notin B_t^{\mathcal{S},\mathcal{I}}) = \left(1 - \frac{\mu(\mathcal{N})}{\mu(\Omega)}\right)^{I_t}. \quad (13)$$

It follows that the probability of \mathbf{x}_t^k being located in an $\mathcal{S} \rightarrow \mathcal{I}$ transition neighborhood is then

$$\mathbb{P}(\mathbf{x}_t^k \in B_t^{\mathcal{S},\mathcal{I}}) = 1 - \left(1 - \frac{\mu(\mathcal{N})}{\mu(\Omega)}\right)^{I_t}. \quad (14)$$

Since $W(\mathcal{S} \rightarrow \mathcal{I})$ depends on cell k being located in at least one infectivity neighborhood, and does not change if cell k is located in more than one infectivity neighborhood, it follows that $W(\mathcal{S} \rightarrow \mathcal{I}) = 1 - \kappa$, where $\kappa \in [0, 1]$ is the contact rate.

⁵ Cell neighborhoods near the boundary will have smaller area, since, by definition, the neighborhood is contained in Ω . However, we assume that since the initially infected cell is located in the center of the region, there are sufficiently many infected cells away from the boundary to make this simplification reasonable.

Then, for any k such that $s_t^k = \mathcal{S}$, by inserting (14) into (10) we have:

$$\begin{aligned}\mathbb{P}(s_{t+1}^k = \mathcal{I}) &= \mathbb{P}(\mathbf{x}_t^k \in B_t^{\mathcal{S}, \mathcal{I}})W(\mathcal{S} \rightarrow \mathcal{I}) \\ &= \left\{ 1 - \left(1 - \frac{\mu(\mathcal{N})}{\mu(\Omega)} \right)^{I_t} \right\} (1 - \kappa).\end{aligned}\quad (15)$$

Moreover, by assuming the cumulative time spent in infected states is uniformly distributed, we have for any cell k such that $s_t^k = \mathcal{I}$:

$$W(\mathcal{I} \rightarrow \mathcal{R}) = 1/T_I, \quad (16)$$

$$W(\mathcal{I} \rightarrow \mathcal{I}) = 1 - 1/T_I, \quad (17)$$

where T_I is the time spent in the infective state. This assumption is valid for a large number of cells and for a sufficiently large number of iterations. Inserting equations (15), (16), and (17) into (10), we have

$$I_{t+1} = (N - I_t - R_t) \left\{ 1 - \left(1 - \frac{\mu(\mathcal{N})}{\mu(\Omega)} \right)^{I_t} \right\} (1 - \kappa) + \left\{ 1 - \frac{1}{T_I} \right\} I_t. \quad (18)$$

That is, the expected number of infected cells at $t+1$ is the sum of two terms. The first term is the product of the expected number of susceptible cells at time t multiplied by the probability a susceptible cell transitions to state \mathcal{I} . The second term is the expected number of infected cells at t times the probability that an infected cell remains in state \mathcal{I} . Similarly, by assuming the time in recovered states is uniformly distributed, we have for any cell k such that $s_t^k = \mathcal{R}$, the probability of staying in state \mathcal{R} is

$$W(\mathcal{R} \rightarrow \mathcal{R}) = 1 - 1/T_R. \quad (19)$$

Then, inserting (16) and (19) into (11) we have

$$R_{t+1} = \frac{1}{T_I} I_t + \left(1 - \frac{1}{T_R} \right) R_t, \quad (20)$$

the expected number of recovered cells at iteration $t+1$ is the sum of two terms. The first term is the expected number of infected cells at time t times the probability an infected cell transitions to state \mathcal{R} . The second term is the expected number of recovered cells at t times the probability a recovered cell remains in state \mathcal{R} .

Since T_I and T_R will be explicitly defined, we can easily find a $q \in \mathbb{R}$ such that $T_R = qT_I$. We then have the following E-CA GRR:

$$I_{t+1} = (N - I_t - R_t) \left\{ 1 - \left(1 - \frac{\mu(\mathcal{N})}{\mu(\Omega)} \right)^{I_t} \right\} (1 - \kappa) + \left(1 - \frac{1}{T_I} \right) I_t := H(I_t, R_t), \quad (21)$$

$$R_{t+1} = \frac{1}{T_I} I_t + \left(1 - \frac{1}{qT_I} \right) R_t := G(I_t, R_t). \quad (22)$$

Since $S_t = N - (I_t + R_t)$, we have recurrence formulas for the expected cell densities in each state at each iteration. With our GRR, we now have a general framework to further analyze the behavior of the system. Note that we identify (21)-(22) as Globally Homogeneous since we have assumed the infectivity neighborhoods are uniformly distributed in the domain with the same constant area.

3.4 Fixed Point Analysis for Globally Homogeneous GRR

We can now calculate the stability of the fixed points of the Globally Homogeneous GRR by finding all solutions to the system that simultaneously solve $I_{t+1} - I_t = 0$ and $R_{t+1} - R_t = 0$. That is, we need to find all solutions to the system

$$\begin{bmatrix} (N - I_t - R_t) \left\{ 1 - (1 - \mu(\mathcal{N}))^{I_t} \right\} (1 - \kappa) - \frac{1}{T_I} I_t \\ \frac{1}{T_I} I_t - \frac{1}{qT_I} R_t \end{bmatrix} = \begin{bmatrix} 0 \\ 0 \end{bmatrix}. \quad (23)$$

We have two fixed points. One is the trivial fixed point, $(I, R) = (0, 0)$. The other is the point along the line $R = qI$ that solves the fixed point problem

$$(N - (1 + q)I) \left\{ 1 - (1 - \mu(\mathcal{N}))^I \right\} (1 - \kappa) - \frac{1}{T_I} I = I. \quad (24)$$

This second fixed point has to be computed numerically.

We will analyze the fixed point $(0, 0)$ using 2-dimensional perturbation theory where details can be found in [11, 19]. Evaluating the Jacobian matrix

of the E-CA GRR at $(0, 0)$ gives us

$$J\Big|_{(I,R)=(0,0)} = \begin{bmatrix} -N(1-\kappa)\ln\left(\frac{\mu(\mathcal{N})}{\mu(\Omega)}\right) - \frac{1}{T_I} & 0 \\ \frac{1}{T_I} & 1 - \frac{1}{qT_I} \end{bmatrix}. \quad (25)$$

The eigenvalues are $\lambda_1 = 1 - \frac{1}{qT_I}$ and $\lambda_2 = -N(1-\kappa)\ln(1 - \frac{\mu(\mathcal{N})}{\mu(\Omega)}) - \frac{1}{T_I}$. Clearly, since $qT_I = T_R > 0$ we know $|\lambda_1| < 1$. Now, suppose $\lambda_2 < 1$. It follows that $\alpha > 1 - \exp\left(\frac{1+1/T_I}{N(1-\kappa)}\right)$. That is, $\frac{\mu(\mathcal{N})}{\mu(\Omega)} > 1 - \exp\left(\frac{1+1/T_I}{N(1-\kappa)}\right)$. We know $\mu(\mathcal{N}) \ll \mu(\Omega)$ and it is reasonable to assume that N is sufficiently large such that $N(1-\kappa) > 2$. This contradicts the inequality. It must follow that $\lambda_2 > 1$. Thus, we have that $(0, 0)$ is a saddle point that is only stable along the nullcline $I = 0$.

Since we do not have an explicit solution of the second fixed point, we cannot perform the same computation as we did for $(0, 0)$. However, since the domain, H , and all the derivatives of H are bounded and since I is repelled by $(0, 0)$, we can infer that the second fixed point is stable.

3.5 Locally Homogeneous Global Recurrence Rule

When deriving the Globally Homogeneous E-CA GRR, (21) and (22), we assumed that infectivity neighborhoods were uniformly distributed throughout Ω . For this test case, we initialize one infected cell, $s_0^1 = \mathcal{I}$, such that it is initially located in the center of the region $\mathbf{x}_0^1 = (0.5, 0.5)$. However, from observation of simulations, such as in Figure 1 (or intuition), we know there is a wave of infectivity propagating from this initial infected cell. The susceptible cells that cell 1 infects must be located in its neighborhood \mathcal{N}^1 . Future infected cells will be located in those neighborhoods. So rather than generalize a uniform distribution of infected cells, we should modify the GRR to account for the infection wave front.

We then need to create a sequence of regions $\{\tilde{B}_0^{S,\mathcal{I}}, \tilde{B}_1^{S,\mathcal{I}}, \dots\}$, where $\tilde{B}_0^{S,\mathcal{I}} = \mathcal{N}^1$ and $\tilde{B}_t^{S,\mathcal{I}}$ is the smallest connected region containing the infection front at time t . For notation, we will use tildes above variables to denote variables and functions specifically defined for the Locally Homogeneous case.

Definition 4. $\tilde{B}_t^{S,\mathcal{I}} = \inf_A \left\{ A \subset \Omega : A \text{ is connected and } \bigcup_{\{k:s_t^k=\mathcal{I}\}} \mathcal{N}_t^k \subset A \right\}$.

Suppose cell k is such that $s_t^k = \mathcal{S}$ at iteration t . We have the following conditional probability that a cell is located in the $\mathcal{S} \rightarrow \mathcal{I}$ transition neighborhood, $B_t^{\mathcal{S},\mathcal{I}}$, given that the cell is within the infection front, $\tilde{B}_t^{\mathcal{S},\mathcal{I}}$:

$$\mathbb{P}\left(\mathbf{x}_t^k \in B_t^{\mathcal{S},\mathcal{I}} \mid \mathbf{x}_t^k \in \tilde{B}_t^{\mathcal{S},\mathcal{I}}\right) = 1 - \left(1 - \frac{\mu(\mathcal{N})}{\mu\left(\tilde{B}_t^{\mathcal{S},\mathcal{I}}\right)}\right)^{I_t}. \quad (26)$$

In general, for regions \mathcal{N} and $\tilde{B}_t^{\mathcal{S},\mathcal{I}}$, the probability is given as $\mathbb{P}\left(\mathbf{x}_t^k \in \tilde{B}_t^{\mathcal{S},\mathcal{I}}\right) = \frac{\mu\left(\tilde{B}_t^{\mathcal{S},\mathcal{I}}\right)}{\mu(\Omega)}$.

Using Bayes' Theorem [33], we have that the Locally Homogeneous probability of a cell being in the $\mathcal{S} \rightarrow \mathcal{I}$ transition neighborhood as

$$\begin{aligned} \mathbb{P}\left(\mathbf{x}_t^k \in B_t^{\mathcal{S},\mathcal{I}}\right) &= \mathbb{P}\left(\mathbf{x}_t^k \in B_t^{\mathcal{S},\mathcal{I}} \mid \mathbf{x}_t^k \in \tilde{B}_t^{\mathcal{S},\mathcal{I}}\right) \mathbb{P}\left(\mathbf{x}_t^k \in \tilde{B}_t^{\mathcal{S},\mathcal{I}}\right), \\ &= \left\{1 - \left(1 - \frac{\mu(\mathcal{N})}{\mu\left(\tilde{B}_t^{\mathcal{S},\mathcal{I}}\right)}\right)^{I_t}\right\} \frac{\mu\left(\tilde{B}_t^{\mathcal{S},\mathcal{I}}\right)}{\mu(\Omega)}. \end{aligned} \quad (27)$$

Inserting (27) into (15), our Locally Homogeneous E-CA GRR is

$$\begin{aligned} \tilde{I}_{t+1} &= \left(N - \tilde{I}_t - \tilde{R}_t\right) \left\{1 - \left(1 - \frac{\mu(\mathcal{N})}{\mu\left(\tilde{B}_t^{\mathcal{S},\mathcal{I}}\right)}\right)^{I_t}\right\} \frac{\mu\left(\tilde{B}_t^{\mathcal{S},\mathcal{I}}\right)}{\mu(\Omega)} (1 - \kappa) \\ &\quad + \left(1 - \frac{1}{T_I}\right) \tilde{I}_t =: \tilde{H}(\tilde{I}_t, \tilde{R}_t), \\ \tilde{R}_{t+1} &= \frac{1}{T_I} \tilde{I}_t + \left(1 - \frac{1}{qT_I}\right) \tilde{R}_t =: \tilde{G}(\tilde{I}_t, \tilde{R}_t). \end{aligned} \quad (28)$$

Recall, the tilde denotes values associated with the Locally Homogeneous GRR.

We derived this GRR by focusing on early dynamics. But how does the non-uniform assumption of the infection front affect the stability using the Locally Homogeneous GRR compared with the Globally Homogeneous GRR?

Theorem 1. *If $\tilde{B}_t^{\mathcal{S},\mathcal{I}} \rightarrow \Omega$ as $t \rightarrow +\infty$ and α is a fixed point of H , then α is a fixed point of \tilde{H} . Moreover, α has the same stability conditions for H and \tilde{H} .*

Proof. Suppose that $\lim_{t \rightarrow +\infty} I_t = \alpha$ and suppose that $\lim_{t \rightarrow +\infty} \tilde{I}_t$ exists. Then, since $\mu\left(\tilde{B}_t^{\mathcal{S}, \mathcal{I}}\right) \rightarrow \mu(\Omega)$ as $t \rightarrow +\infty$, we have that

$$\lim_{t \rightarrow +\infty} \left(1 - \frac{\mu(\mathcal{N})}{\mu\left(\tilde{B}_t^{\mathcal{S}, \mathcal{I}}\right)}\right)^{\tilde{I}_t} = \lim_{t \rightarrow +\infty} \left(1 - \frac{\mu(\mathcal{N})}{\mu(\Omega)}\right)^{\tilde{I}_t}.$$

Plugging into the equation (21) for H and taking the limit,

$$\begin{aligned} \lim_{t \rightarrow +\infty} \tilde{H}(\tilde{I}_t) &= \lim_{t \rightarrow +\infty} \left[(N - \tilde{I}_t) \left(1 - \frac{\mu(\mathcal{N})}{\mu(\Omega)}\right)^{\tilde{I}_t} (1 - \kappa) + \left(1 - \frac{1}{qT_I}\right) \tilde{I}_t \right] \\ &= \lim_{t \rightarrow +\infty} H(\tilde{I}_t) = \alpha. \end{aligned}$$

Moreover, we have the following partial derivatives: Since $\mu(\tilde{B}_{\mathcal{S}, \mathcal{I}}^t) \rightarrow \mu(\Omega)$, for fixed α , it is clear that $\left.\frac{\partial \tilde{H}}{\partial I}\right|_{\alpha} \rightarrow \left.\frac{\partial H}{\partial I}\right|_{\alpha}$, $\left.\frac{\partial \tilde{H}}{\partial R}\right|_{\alpha} \rightarrow \left.\frac{\partial H}{\partial R}\right|_{\alpha}$, $\left.\frac{\partial \tilde{G}}{\partial I}\right|_{\alpha} \rightarrow \left.\frac{\partial G}{\partial I}\right|_{\alpha}$, and $\left.\frac{\partial \tilde{G}}{\partial R}\right|_{\alpha} \rightarrow \left.\frac{\partial G}{\partial R}\right|_{\alpha}$. Since the stability condition depends on the Jacobian, and the Jacobian of the Locally Homogeneous region approaches the Jacobian of the Globally Homogeneous region as $t \rightarrow +\infty$, the long term stability conditions must be the same. \square

From Theorem 1 we know that (\tilde{H}, \tilde{G}) has the same fixed points as found in Section 3.4 with the same stability conditions. We thus reduced the problem to capturing an explicit formula for $\mu\left(\tilde{B}_t^{\mathcal{S}, \mathcal{I}}\right)$. Before, we made the simplifying assumption that the infected cells were distributed uniformly throughout the region, so we did not need to incorporate any spatial characteristics into the Globally Homogeneous GRR. Now, we need to capture the infection front dynamics in order to explicitly calculate the area of the infectivity region, $\mu\left(\tilde{B}_t^{\mathcal{S}, \mathcal{I}}\right)$, in the Locally Homogeneous case.

For our formula, we will assume that newly infected cells are expected to be in the region $\tilde{B}_t^{\mathcal{S}, \mathcal{I}} \setminus \tilde{B}_{t-1}^{\mathcal{S}, \mathcal{I}}$ and are moving a fixed distance Δr . Further, we assume the expected location of the newly infected cells will lie on the circle that is the radial center of mass of $\tilde{B}_t^{\mathcal{S}, \mathcal{I}} \setminus \tilde{B}_{t-1}^{\mathcal{S}, \mathcal{I}}$, a distance r from the initially infected cell location as shown in Figure 2. The radius of the infectivity front region $\tilde{B}_t^{\mathcal{S}, \mathcal{I}}$ at time t is denoted as ζ_t . We then have the following expected radius of $\tilde{B}_{t+1}^{\mathcal{S}, \mathcal{I}}$,

$$\zeta_{t+1} = \rho_0 + \sqrt{\frac{(\zeta_t + \delta_{out}(\Delta r))^2 + (\zeta_{t-1} - \delta_{in}(\Delta r))^2}{2}}, \quad (29)$$

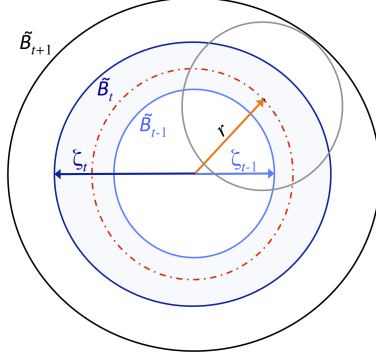


Figure 2: Diagram demonstrating how the Locally Homogeneous $\tilde{B}_{t+1}^{\mathcal{S}, \mathcal{I}}$ region depends on $\tilde{B}_t^{\mathcal{S}, \mathcal{I}}$ and $\tilde{B}_{t-1}^{\mathcal{S}, \mathcal{I}}$ regions. The initially infected cell at $t = 0$ is located in the center of the $\tilde{B}_t^{\mathcal{S}, \mathcal{I}}$ regions, which expand outwards with radii ζ_t . We assume newly infected cells lie on the radial center of mass of the region $\tilde{B}_t^{\mathcal{S}, \mathcal{I}} \setminus \tilde{B}_{t-1}^{\mathcal{S}, \mathcal{I}}$, denoted with the dashed line, which is a distance r from the initially infected cell.

where δ_{in} and δ_{out} are functions of the expected distance an infected cell travels towards the center of $\tilde{B}_t^{\mathcal{S}, \mathcal{I}}$ and out of the region $\tilde{B}_t^{\mathcal{S}, \mathcal{I}}$, respectively. For our simulations and derivation, we assume $\delta_{out} = \Delta r$ and $\delta_{in} = \Delta r$. Even though the simulation is a Markov process, our analytical solution, which calculates the area $\mu(\tilde{B}_{t+1}^{\mathcal{S}, \mathcal{I}})$ using ζ_{t+1} is not, since it relies on information at iterations t and $t - 1$. Clearly, the simulation is a Markovian process but the GRR does not have to be for this analysis. In fact, it can belong to a larger class of processes than the underlying CA or AB model.

By the following theorem, we know that equation (29) satisfies the premise of Theorem 1.

Theorem 2. *If $\rho_0 > 0$ and $\forall j$ such that $\mu(\tilde{B}_j^{\mathcal{S}, \mathcal{I}}) \neq \mu(\Omega)$ there exists a cell k with $s_j^k = \mathcal{S}$ such that $\mathbf{x}_j^k \notin \tilde{B}_j^{\mathcal{S}, \mathcal{I}}$, then $\exists \hat{t} \in \mathbb{N}$ such that $\mu(\tilde{B}_t^{\mathcal{S}, \mathcal{I}}) = \mu(\Omega)$ for all $t > \hat{t}$ with radius ζ_t as defined in (29).*

The above theorem essentially states that if the infection does not “die out,” then the $\mathcal{S} \rightarrow \mathcal{I}$ transition neighborhood, $\tilde{B}_j^{\mathcal{S}, \mathcal{I}}$, eventually covers the entire region of interest Ω . The proof is clear, since Ω is bounded. As we will see in Section 4, we are able to approximate early behavior more accurately with the Locally Homogeneous GRR, while still being able to evaluate and

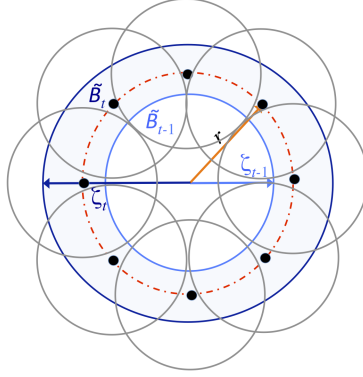


Figure 3: Infectivity neighborhood depends on the number n of newly infected cells. The radial center of mass of the region $\tilde{B}_t^{S,I} \setminus \tilde{B}_{t-1}^{S,I}$ (dashed line) is a distance r from the initially infected cell. Newly infected cells are distributed uniformly along the radial center of mass and the new infection front radius ζ_{t+1} will depend on the total area of the infectivity neighborhoods outside $\tilde{B}_t^{S,I}$.

determine the stability of fixed points with the simpler equations of the Globally Homogeneous GRR.

3.6 Extensions To More Complex Neighborhoods

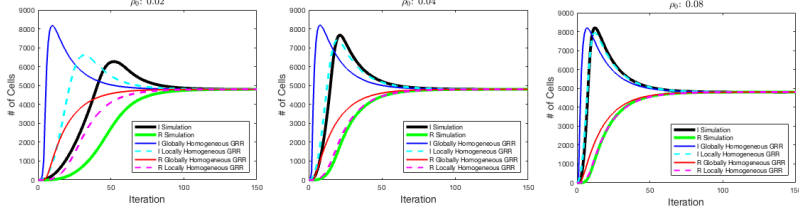
As long as the infection front in the E-CA approaches $\partial\Omega$ and $\tilde{B}_t^{S,I} \rightarrow \partial\Omega$, Theorem 1 holds. One could derive a formula for $\tilde{B}_t^{S,I}$ that more closely approximates the initial phases of the infection spread. Rather than assume that the new infection front extends approximately Δr from the mean center of mass as in Figure 2, we can assume that the infectivity radius expansion depends on the number of newly infected cells in $\tilde{B}_t^{S,I} \setminus \tilde{B}_{t-1}^{S,I}$, as shown in Figure 3.

Further details regarding the calculation and derivation for this case of $\tilde{B}_t^{S,I}$ can be found in Appendix B. In this example, we illustrate that, by relaxing assumptions, one can derive other expressions calculating the area of the infectivity front radius ζ_t that may decrease the error of the Locally Homogeneous GRR during the early stages of the epidemic. Moreover, we know that as long as the new formulation of ζ_t maintains the suppositions of Theorem 1, the long term dynamics will be captured.

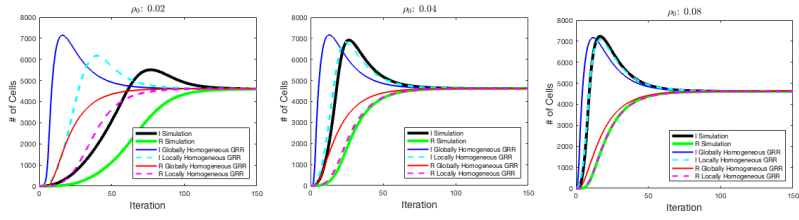
4 Numerical Results

Results for the epidemiological model with $N = 10000$ initialized cells are shown in Figure 4. Note that each simulation curve on the plot is the average of 1000 E-CA simulations whereas the curves based on the Globally and Locally Homogeneous GRRs are from solving (22) and (28), respectively. In the Figure, we observe agreement of long term behavior of the simulations with both the Globally and Locally Homogeneous GRRs. For example, in Figure 4c, the left hand graph corresponds to the case where $\rho_0 = 0.02$. The average of the E-CA simulations for the fixed points or long term behavior is 3877.1 infected cells and 5790.9 recovered cells. Upon calculation, the relative error between the simulated fixed points and the GRR fixed points are $\mathcal{O}(10^{-4})$. Further, the early time dynamics of the infected and recovered populations with the GRR estimates have similar behavior to that of the E-CA simulations.

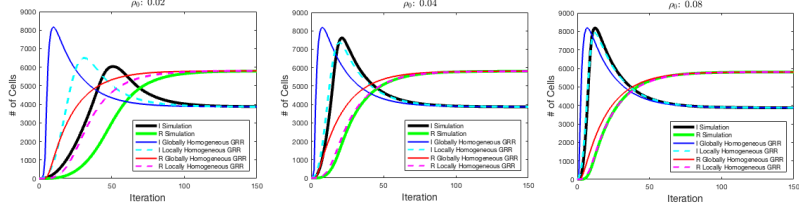
However, the early infection dynamics of the GRRs do not exactly match the simulations for all cases. In Figure 4(a)-(b), for a contact tolerance $\kappa = 0.6$ and $\kappa = 0.8$ (characterizing how easily a cell becomes infected), we observe that as the infectivity radius increases, the GRRs are able to more accurately capture the early time dynamics of the E-CA simulations. For an infectivity neighborhood of radius $\rho_0 = 0.02$, it is likely that there is not a sufficient number of cells in the region to accurately capture the early time dynamics of infectivity. We do observe that the Locally Homogeneous GRR provides a better approximation to the E-CA simulations in comparison to the Globally Homogeneous GRR. Similar trends are observed in Figure 4(c)-(d) where the recovery time T_R is increased. To explicitly define how much “better” the Locally Homogeneous GRR is relative to the Globally Homogeneous GRR at capturing the E-CA dynamics for a particular parameter set, we need to develop a metric. We have a sequence of points, $(1, U_1), (2, U_2), \dots, (M, U_M)$, from the simulation, where U_t , as previously defined, is the number of cells in state \mathcal{U} at iteration t for $t = 1, \dots, M$. By linear spline interpolation of these points we will construct a function $g(t)$. We also have a sequence of points, $(1, \hat{U}_1), (2, \hat{U}_2), \dots, (M, \hat{U}_M)$, from the GRR. Given the fact that some of the error is due to translation and that the number of cells is much larger than the number of iterations, we need to normalize the data. We scale the t -values so that $t_i \leftarrow t_i/M$ and $\hat{t}_i \leftarrow \hat{t}_i/M$. Additionally, we let $\gamma = \max\{U_1, U_2, \dots, U_M\}$ and scale the U -values so that $U_i \leftarrow U_i/\gamma$ and $\hat{U}_i \leftarrow \hat{U}_i/\gamma$. Our error metric ν in Equation (30) is a nor-



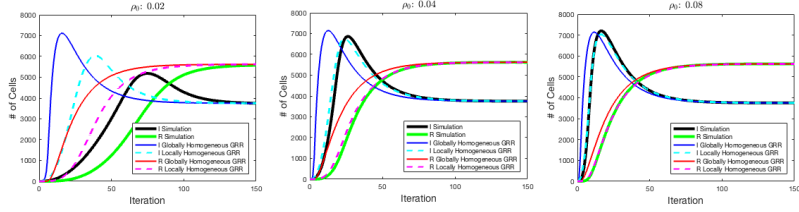
(a) $N = 10000, \kappa = 0.6, T_I = T_R = 30$



(b) $N = 10000, \kappa = 0.8, T_I = T_R = 30$



(c) $N = 10000, \kappa = 0.6, T_I = 30, T_R = 45$



(d) $N = 10000, \kappa = 0.8, T_I = 30, T_R = 45$

Figure 4: Comparing the average value of 1000 E-CA simulations with results from the Globally and Locally Homogeneous Global Recurrence Rules calculated from (22) and (28), respectively. The time to remain infected is set to $T_I = 30$, while the recovery time is $T_R = 30$ in (a)-(b) and $T_R = 45$ in (c)-(d). Each plot corresponds to a different infectivity radii parameter ρ_i with contact tolerance $\kappa = 0.6$ in (a), (c) and $\kappa = 0.8$ in (b), (d).

malized least square, evaluating the average distance of each scaled GRR estimation to the scaled E-CA simulated curve. Details of the derivation for the error metric can be found in Appendix A.

Table 1: Error between GRR and 1000 E-CA simulations using metric ν from Equation (30) for infectivity radii ρ_0 , contact tolerances κ , time in infected state T_I , and time in recovered state T_R .

(a) Error for number of infected cells.

$N = 10000$	$T_I = T_R = 30$				$T_I = 30, T_R = 45$			
	$\kappa = 0.6$		$\kappa = 0.8$		$\kappa = 0.6$		$\kappa = 0.8$	
	Global	Local	Global	Local	Global	Local	Global	Local
$\rho_0 = 0.02$	0.036606	0.009573	0.052660	0.020494	0.035438	0.010552	0.059061	0.021560
$\rho_0 = 0.04$	0.008092	0.001398	0.007514	0.001237	0.008595	0.001687	0.008653	0.001444
$\rho_0 = 0.08$	0.004019	0.000652	0.003252	0.000360	0.004686	0.000692	0.003657	0.000391
$\rho_0 = 0.16$	0.002030	0.000798	0.001589	0.000545	0.002352	0.000859	0.001827	0.000608

(b) Error for number of recovered cells.

$N = 10000$	$T_I = T_R = 30$				$T_I = 30, T_R = 45$			
	$\kappa = 0.6$		$\kappa = 0.8$		$\kappa = 0.6$		$\kappa = 0.8$	
	Global	Local	Global	Local	Global	Local	Global	Local
$\rho_0 = 0.02$	0.022055	0.009537	0.027853	0.015889	0.028273	0.012485	0.036781	0.021142
$\rho_0 = 0.04$	0.008436	0.000831	0.008046	0.000817	0.010412	0.000895	0.010120	0.000937
$\rho_0 = 0.08$	0.003581	0.000126	0.003084	0.000104	0.004247	0.000138	0.003694	0.000103
$\rho_0 = 0.16$	0.001247	0.000176	0.001117	0.000154	0.001350	0.000189	0.001260	0.000184

We see from Figure 4, as well as Table 1a and Table 1b, that the Locally Homogeneous GRR approaches the E-CA with less error than the Global GRR. Despite the scaling and translation differences, the general behavioral trends of the Global GRR and Locally Homogeneous GRR emulate the E-CA cell state densities.

The surface plot in Figure 5 shows the mean error between the Locally Homogeneous GRR and the E-CA simulations with respect to the number of infected individuals. The horizontal axis represents the expected number of susceptible cells in the initial infected cell's neighborhood and the vertical axis represents the contact tolerance κ for the mean error calculated from (30) using 150 iterations of data. We fixed the number of cells, N , and varied the infectivity radius, ρ_0 to generate the error surface plot in Figure 5, however one can generate similar error surface plots by fixing N and varying ρ_0 .

Regardless of the contact tolerance κ , the GRR approaches the mean simulation's fixed point with only two expected susceptible cells in the initial infected cell's neighborhood — the lower left subplot *does* approach the

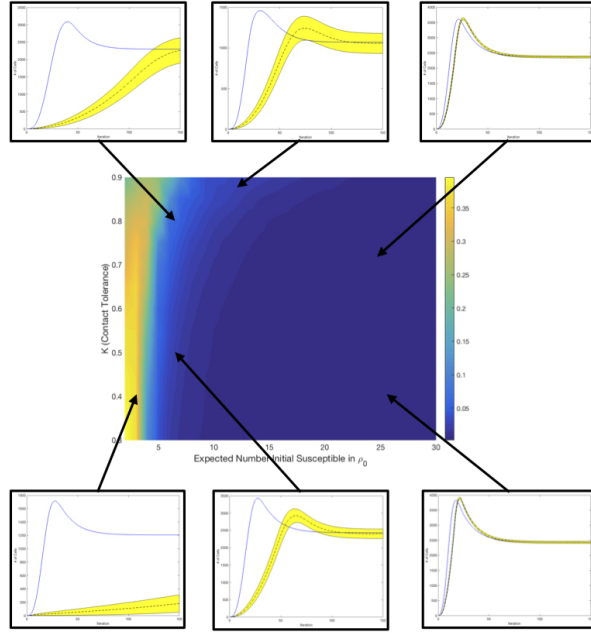


Figure 5: The surface plot in the center displays the error between the Locally Homogeneous GRR and the E-CA simulations with respect to the number of infected cells as a function of the contact tolerance and the expected number of susceptible cells located in the initial infected cell’s neighborhood at $t = 0$. The 6 outside plots show the Locally Homogeneous GRR infected population solution (blue) and the simulated solution (black) with a bound of \pm one standard deviation (yellow).

fixed point when the simulation runs for more iterations. However, the early infection front is better captured as the density of cells in the initial infectivity radius increases, as shown in the dark blue bands in the surface plot in Figure 5. In the yellow and orange bands of the surface plot (approximately fewer than 4 susceptible cells in the initial infectivity radius), we find that in some simulations the infected cells transition to recovered before any susceptible cells become infected, reaching a point early in the epidemic where there are no infected cells. These cases, in which the epidemic “dies out,” skews the expected number of infected, leading to higher error. The number of iterations required to match depends inversely on the expected number of susceptible cells in the initial infectivity radius. For very low density simulations, where fewer than 2 susceptible cells are expected to be in the initial

infectivity radius, the epidemic has a greater chance of “dying out,” which makes our current analysis unreliable.

5 Discussion & Conclusions

In this paper we have introduced a Global Recurrence Rule (GRR) for estimating the state densities for each iteration of a Markovian off-lattice CA or AB model. We demonstrated its utility with a three state epidemiological Cellular Automata (E-CA) model. Using the GRR, we were able to perform stability analysis on the E-CA, as well as determine bounds for the efficacy of the GRR in early stages of the epidemic. We note that other analytical techniques, besides stability analysis, can be explored with the GRR, including parameter sensitivity analysis and parameter estimation. Performing these calculations directly with a CA or AB model would prove to be very computationally expensive. But, with the computational efficiency of the GRR, one could take existing epidemic data and find the E-CA parameters that best-fit the data. It is well known that the ease of quick and simple calibration of an AB or CA model is critical [29], and this methodology provides a framework to easily handle parameter sweeps.

We identified two classes of E-CA GRR: a Globally Homogeneous GRR, which assumes that the infected cells are uniformly distributed throughout the domain, and a Locally Homogeneous GRR, which assumes that there is an infectivity front expanding outward from the initially infected cell. Although an AB or CA model is a Markovian process, we found that the GRR can belong to a larger class of processes—which is the case with the Locally Homogeneous GRR. With relaxed assumptions, the Locally Homogeneous GRR performs better than the Globally Homogeneous GRR with respect to early epidemic prediction. However, we demonstrated and proved that the much simplified Globally Homogeneous GRR can predict long-term behavior just as well as the Locally Homogeneous GRR.

Further, we demonstrated that the GRR is a generalized model, but is not unique in its application — certain choices must be made. The generalized GRR definition lends itself to be used as a framework when adapting similar models. For example, if the E-CA were three-dimensional or if the neighborhoods were a different geometry, then we could use our previously derived GRR equations 21, 22, and 28 while only simply having to derive new expressions for $\mu(\mathcal{N})$ and ζ_t . Further, we assumed a constant number of

cells, N , but we could derive a GRR to calculate S_t , I_t , and R_t that incorporates a dynamically varying number of agents in much the same way as we did in Section 3. The analysis would be similar, only in three-dimensional phase space instead of two-dimensional.

Previous analytical techniques, such as mean-field game theory, assume the density of agents approaches infinity in order to calculate end behavior [17]. Other approaches take continuum limits to approximate the dynamics of AB or CA cellular distributions as a system of PDEs [7, 12, 25]; which often corresponds to reducing the scales to infinitesimal time or spatial steps. In contrast, the GRR analysis allows for and takes into account a finite number of agents in a discrete spatial and temporal domain, which in some cases might more closely reflect the outcome of interest for a particular application.

Our explicit GRR formulation for the E-CA model ultimately fails when the density of the infected population is zero. In general, the expansion of the wave of infectivity is caused by the infection spread, rather than the cell movement. However, when cell density is low, the early infectivity front growth relies on cell movement. For the infection to not “die out” in these cases, we require an increase in the ratio of the movement size to the neighborhood area to increase the probability that a susceptible cell encounters the infectivity region. In the future, we will develop continuum approximations of state changes in order to determine the probability that an infection will “die out.” These will establish density and parameter bounds for when the E-CA GRR formulation is reliable. Early predictions of disease dynamics are necessary [27, 30], and the proposed framework can be extended to determine accuracy of these estimates for given parameter regimes.

6 Acknowledgments

S.D. Olson and M.A. Yereniuk were funded, in part, by NSF 1455270.

A Derivation of Metric

Suppose we create a linear spline interpolant $f(t)$ from a sequence of points $(t_1, S_1), (t_2, S_2), \dots, (t_N, S_M)$. Suppose we also have another sequence of points $(\hat{t}_1, \hat{S}_1), (\hat{t}_2, \hat{S}_2), \dots, (\hat{t}_M, \hat{S}_M)$. Our error metric is a normalized least square,

$$\nu = \frac{1}{M} \sum_{k=1}^M \inf_t \sqrt{(\hat{t}_k - t)^2 + (\hat{S}_k - f(t))^2}, \quad (30)$$

where our spline interpolation [32] is $f(t) = \frac{S_{k+1} - S_k}{t_{k+1} - t_k}(t - t_k) + S_k$, for $t_k \leq t \leq t_{k+1}$.

Consider a point (\hat{t}, \hat{S}) . We want to find

$d(\hat{\mathbf{x}}, f) = \inf_t \sqrt{(\hat{t} - t)^2 + (\hat{S} - f(t))^2}$. The line that intersects points (t_k, S_k) and (t_{k+1}, S_{k+1}) is given by

$$\ell_k := S = \frac{S_{k+1} - S_k}{t_{k+1} - t_k}(t - t_k) + S_k. \quad (31)$$

To find X such that $d(\hat{\mathbf{x}}, \ell_k)$ is minimized we find the line $\hat{\ell}$ that intersects $\hat{\mathbf{x}}$ and ℓ_k . This line is given by

$$\hat{\ell} := S = -\frac{t_{k+1} - t_k}{S_{k+1} - S_k}(t - \hat{t}) + \hat{S}. \quad (32)$$

Setting (31) and (32) equal and solving for t we find that

$$X = \frac{(t_{k+1} - t_k)(S_{k+1} - S_k)}{(t_{k+1} - t_k)^2 + (S_{k+1} - S_k)^2} \left(\frac{t_{k+1} - t_k}{S_{k+1} - S_k} \hat{t} + \frac{S_{k+1} - S_k}{t_{k+1} - t_k} t_k + \hat{S} - S_k \right). \quad (33)$$

It follows that $Y = \ell_k(X)$. We then calculate

$$d_k = \begin{cases} \sqrt{(\hat{t} - t_k)^2 + (\hat{S} - S_k)^2} & : \text{if } X < t_k \\ \sqrt{(\hat{t} - t_{k+1})^2 + (\hat{S} - S_{k+1})^2} & : \text{if } S_{k+1} < X \\ \sqrt{(X - S_k)^2 + (Y - S_{k+1})^2} & : \text{otherwise} \end{cases} \quad (34)$$

We then have that $d(\hat{\mathbf{x}}, f) = \inf_t \sqrt{(\hat{t} - t)^2 + (\hat{S} - f(t))^2} = \min\{d_1, d_2, \dots, d_{N-1}\}$. It follows that we calculate the Error by $\nu = \sum_{k=1}^M d(\hat{\mathbf{x}}_k, f)$.

B Sparse $\mu\left(\tilde{B}_t^{\mathcal{S},\mathcal{I}}\right)$ Formula

Let us assume, as we did when deriving the Locally Homogeneous region, that the infected cells are on the radial center of mass of the region $\tilde{B}_t^{\mathcal{S},\mathcal{I}} \setminus \tilde{B}_{t-1}^{\mathcal{S},\mathcal{I}}$, as shown in Figure 3. We will assume that there are n newly infected cells that are uniformly distributed on the radial center of mass, a distance of r from the initially infected cell.

B.1 Deriving ζ_{k+1}

We want to find the total area $\mu\left(\bigcup_{i=1}^n A_i\right)$, where n is the expected number of infected cells in the region $\tilde{B}_t^{\mathcal{S},\mathcal{I}} \setminus \tilde{B}_{t-1}^{\mathcal{S},\mathcal{I}}$ and A_i is the region, illustrated in Figure 3, of the i th infected cell. For our expository purposes, we will assume the simplified derivation, $n = I_t - I_{t-1}$.

By the Inclusion-Exclusion principle [34] we find that $\mu\left(\bigcup_{i=1}^n A_i\right) = \sum_{i=1}^n \mu(A_i) - \sum_{i=1}^n \mu(A_i \cap A_{i+1})$, where $A_{n+1} = A_1$. Note that $\mu(A_i) = \mu(A_j)$ and that $\mu(A_i \cap A_{i+1}) = \mu(A_j \cap A_{j+1})$ for all $i, j = 1, 2, \dots, n$. We then have that

$$\mu\left(\bigcup_{i=1}^n A_i\right) = n(\mu(A) - \mu(A_1 \cap A_2)). \quad (35)$$

First we will find $\mu(A)$, the region shown in Figure 6a.

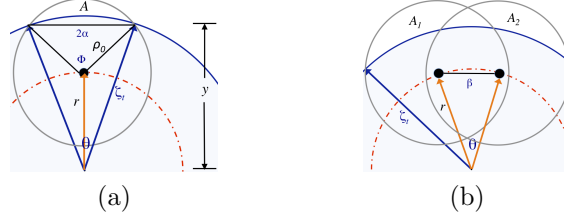


Figure 6: Newly infected cells (black circles) lie on the radial center of mass of the region $\tilde{B}_t^{\mathcal{S},\mathcal{I}} \setminus \tilde{B}_{t-1}^{\mathcal{S},\mathcal{I}}$, a distance r from the initially infected cell. Left: Solving for $\mu(A)$ as part of calculating how large the infection front becomes. The infectivity radius of the cell intersects the edge of region $\tilde{B}_t^{\mathcal{S},\mathcal{I}}$ at 2 points creating an angle θ from the center of the region and an angle Φ from the cell. Right: Solving for $\mu(A_1) \cap \mu(A_2)$. The infected cells are a distance β apart and form an angle θ from the center of the region $\tilde{B}_t^{\mathcal{S},\mathcal{I}}$.

We already know r and ζ_t . By our assumption, $\theta = 2\pi/n$, we will find y by finding the intersection of C_1 and C_2 defined by

$$\begin{aligned} C_1 : x^2 + (y - r)^2 &= \rho_0^2, \\ C_2 : x^2 + y^2 &= \zeta_t^2. \end{aligned}$$

It follows that $y = \frac{\zeta_t^2 - \rho_0^2 + r^2}{2r}$. We can then find $\alpha = \sqrt{\zeta_t^2 - y^2}$ and $\Phi = 2 \arcsin\left(\frac{\alpha}{\rho_0}\right)$.

From Figure 7 we know that $\mu(A) = \mu(R_2) - \mu(R_4)$. It is clear that $\mu(R_2) = \mu(R_1 \cup R_2) - \mu(R_1) = \frac{\Phi}{2}\rho_0^2 - \alpha\sqrt{\rho_0^2 - \alpha^2}$ and $\mu(R_4) = \mu(R_3 \cup R_4) - \mu(R_3) = \frac{\theta}{2}\zeta_t^2 - \alpha y$.

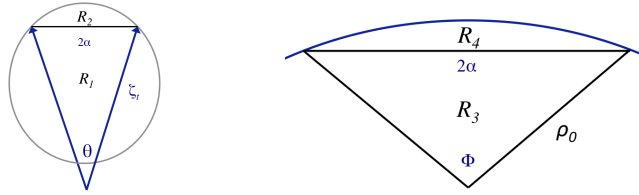


Figure 7: We solve for region A by subtracting $\mu(R_4)$ from $\mu(R_2)$. We decompose solving for $\mu(A)$ in Figure 6a by solving for the outer sector (left) and the inner sector (right).

We then have that

$$\mu(A) = \frac{1}{2} (\Phi \rho_0^2 - \theta \zeta_t^2) - \alpha \left(\sqrt{\rho_0^2 - \alpha^2 - y} \right). \quad (36)$$

Now we will find $\mu(A_1) \cap \mu(A_2)$. From Figure 6b we know θ , r , and ζ_t . We want to find the x-coordinate of the intersection of C_1 and C_2 defined as:

$$\begin{aligned} C_1 : (x + h)^2 + (y - k)^2 &= \rho_0^2, \\ C_2 : x^2 + y^2 &= \zeta_t^2 \end{aligned}$$

with $h = \beta/2$ and $k = \sqrt{r^2 - (\beta/2)^2}$. The intersection is the larger solution \hat{x} of the quadratic $4(h^2 + k^2)\hat{x}^2 + 4h(2k^2 + \eta)\hat{x} + (\eta^2 - 4k^2(\rho_0^2 - h^2)) = 0$, where $\eta = h^2 - k^2 + \zeta_k^2 - \rho_0^2$.

We then have that

$$\mu(A_1 \cap A_2) = 2 \int_0^{\hat{x}} \left(k + \sqrt{\rho_0^2 - (x + h)^2} - \sqrt{\zeta_t^2 - x^2} \right) dx,$$

if $\hat{x} > 0$. After integrating, if $\hat{x} > 0$ we have

$$\begin{aligned} \mu(A_1 \cap A_2) &= (h + \hat{x})\sqrt{\rho_0^2 - (h + \hat{x})^2} + \rho_0^2 \arctan \left(\frac{h + \hat{x}}{\sqrt{\rho_0^2 - (h + \hat{x})^2}} \right) \\ &\quad - \zeta_t^2 \arctan \left(\frac{\hat{x}}{\sqrt{\zeta_t^2 - \hat{x}^2}} \right) - \hat{x}\sqrt{\zeta_t^2 - \hat{x}^2} + 2k\hat{x} \\ &\quad - \left[h\sqrt{\rho_0^2 - h^2} + \rho_0 \arctan \left(\frac{h}{\sqrt{\rho_0^2 - h^2}} \right) \right] \end{aligned} \quad (37)$$

After inserting equations (36) and (37) into equation (35), we have a computable formula for $\mu(\cup_{k=1}^n A_k)$. Our new wavefront radius is:

$$\zeta_{t+1} = \sqrt{\frac{\pi \zeta_t^2 + \mu(\cup_{i=1}^n A_i)}{\pi}}. \quad (38)$$

The above formulation works well for low density E-CA simulations, where cells in state \mathcal{R} do not return to state \mathcal{S} (T_R is longer than the time of the simulation). However, if recovered cells can become susceptible then we must reformulate our calculation of the expected value of n .

References

- [1] G. An, B. G. Fitzpatrick, S. Christley, P. Federico, A. Kanarek, R. Miller Neilan, M. Oremland, R. Salinas, R. Laubenbacher, and S. Lenhart. Optimization and control of agent-based models in biology: A perspective. *Bull. Math. Biol.*, 79(1):63–87, 2017.
- [2] Frank Ball, Tom Britton, Thomas House, Valerie Isham, Denis Mollison, Lorenzo Pellis, and Gianpaolo Scalia Tomba. Seven challenges for metapopulation models of epidemics, including households models. *Epidemics*, 10:63 – 67, 2015. Challenges in Modelling Infectious Disease Dynamics.
- [3] Eric Bonabeau. Agent-based modeling: Methods and techniques for simulating human systems. *Proc. Natl. Acad. Sci. U.S.A.*, 99(suppl 3):7280–7287, 2002.
- [4] M. Burkitt, D. Walker, D.M. Romano, and A. Fazeli. Constructing complex 3d biological environments from medical imaging using high performance computing. *IEEE Transac. Computat. Bio. Bioinf.*, 9:643–654, 2012.
- [5] M. Burkitt, D. Walker, D.M. Romano, and A. Fazeli. Using computational modeling to investigate sperm navigation and behavior in the female reproductive tract. *Theriogenology*, 77:703–716, 2012.
- [6] Doran Chakraborty, SpringerLink (Online service), and Springer Books. *Sample Efficient Multiagent Learning in the Presence of Markovian Agents*. Springer International Publishing, 2014th edition, 2014.
- [7] Sorathan Chaturapruek, Jonah Breslau, Daniel Yazdi, Theodore Kolkolnikov, and Scott G. McCalla. Crime modeling with lévy flights. *SIAM J. Appl. Math.*, 73(4):1703–1720, 2013.
- [8] Qiuwen Chen, Jingqiao Mao, and Weifeng Li. Stability analysis of harvesting strategies in a cellular automata based predator-prey model. In Samira El Yacoubi, Bastien Chopard, and Stefania Bandini, editors, *Cellular Automata*, pages 268–276, Berlin, Heidelberg, 2006. Springer Berlin Heidelberg.

- [9] J Cosgrove, J Butler, K Alden, M Read, V Kumar, L Cucurull-Sanchez, J Timmis, and M Coles. Agent-based modeling in systems pharmacology. *CPT Pharmacometrics Syst. Pharmacol.*, 4(11):615–629, 2015.
- [10] Burgess Davis. Reinforced random walk. *Probab. Theory Relat. Fields*, 84(2):203–229, 1990.
- [11] Andreas Deutsch and Sabine Dormann. *Cellular Automaton Modeling of Biological Pattern Formation*. Birkhäuser, Boston, 2nd edition, 2005.
- [12] Adrian Devitt-Lee, Hongyan Wang, Jie Li, and Bruce Boghosian. A non-standard description of wealth concentration in large-scale economies. *SIAM J. Appl. Math.*, 78(2):996–1008, 2018.
- [13] Guillermo H. Goldsztein. Particles moving around a two-lane circular track in both directions. avoiding collisions leads to self-organization. *SIAM J. Appl. Math.*, 76(4):1433–1445, 2016.
- [14] Franziska Hinkelmann, David Murrugarra, Abdul Salam Jarrah, and Reinhard Laubenbacher. A mathematical framework for agent based models of complex biological networks. *Bull. Math. Biol.*, 73(7):1583–1602, 2011.
- [15] Mike Holcombe, Salem Adra, Mesude Bicak, Shawn Chin, Simon Coakley, Alison I. Graham, Jeffrey Green, Chris Greenough, Duncan Jackson, Mariam Kiran, Sheila MacNeil, Afsaneh Maleki-Dizaji, Phil McMinn, Mark Pogson, Robert Poole, Eva Qwarnstrom, Francis Ratnieks, Matthew D. Rolfe, Rod Smallwood, Tao Sun, and David Worth. Modelling complex biological systems using an agent-based approach. *Integr. Biol.*, 4:53–64, 2012.
- [16] Ruben Interian, Reinaldo Rodriguez-Ramos, Fernando Valdeis-Ravelo, Ariel Ramirez-Torres, Celso C. Ribeiro, and Aura Conci. Tumor growth modelling by cellular automata. *MEMOCS*, 5(3-4):239–259, 2017.
- [17] J. Lasry and P. Lions. Mean field games. *Jap. J. Math.*, 2(1):229–260, 2007.
- [18] Reinhard Laubenbacher, Abdul S. Jarrah, Henning S. Mortveit, and S.S. Ravi. Mathematical formalism for agent based modeling. In Robert A.

- Meyers, editor, *Computational Complexity: Theory, Techniques, and Applications*, pages 88–104. Springer New York, New York, NY, 2012.
- [19] C.C. Lin and L.A. Segel. *Mathematics Applied to Deterministic Problems in the Natural Sciences*, chapter 11, pages 321–345. Society for Industrial and Applied Mathematics, Philadelphia, 1 edition, 1988.
- [20] A.L. Lloyd. Realistic distributions of infectious periods in epidemic models: Changing patterns of persistence and dynamics. *Theor. Popul. Biol.*, 60(1):59–71, 2001.
- [21] J. Ma and D.J.D. Earn. Generality of the final size formula for an epidemic of a newly invading infectious disease. *Bull. Math. Biol.*, 68(3):679–702, 2006.
- [22] Valentina Marziano, Andrea Pugliese, Stefano Merler, and Marco Ajelli. Detecting a surprisingly low transmission distance in the early phase of the 2009 influenza pandemic. *Sci. Rep.*, 7(1), 2016.
- [23] J.C. Miller. A note on the derivation of epidemic final sizes. *Bull. Math. Biol.*, 74(9):2125–2141, 2012.
- [24] Michael J. North. A theoretical formalism for analyzing agent-based models. *CASM*, 2(1):3, 2014.
- [25] Hans G. Othmer and Angela Stevens. Aggregation, blowup, and collapse: The abc’s of taxis in reinforced random walks. *SIAM J. Appl. Math.*, 57(4):1044–1081, 1997.
- [26] Norman H. Packard and Stephen Wolfram. Two-dimensional cellular automata. *J. Stat. Phys.*, 38(5):901–946, 1985.
- [27] Lorenzo Pellis, Frank Ball, Ken Eames, Thomas House, Valerie Isham, and Pieter Trapman. Eight challenges for network epidemic models. *Epidemics*, 10:58 – 62, 2015.
- [28] Mark Pogson, Rod Smallwood, Eva Qwarnstrom, and Mike Holcombe. Formal agent-based modelling of intracellular chemical interactions. *Biosystems*, 85(1):37 – 45, 2006. Dedicated to the Memory of Ray Paton.

- [29] D. Prieto and T. K. Das. An operational epidemiological model for calibrating agent-based simulations of pandemic influenza outbreaks. *Health Care Manag. Sc.*, 19(1):1–19, 2016.
- [30] Mick Roberts, Viggo Andreasen, Alun Lloyd, and Lorenzo Pellis. Nine challenges for deterministic epidemic models. *Epidemics*, 10(7):49 – 53, 2015.
- [31] Angela Stevens. A stochastic cellular automaton modeling gliding and aggregation of myxobacteria. *SIAM J. Appl. Math.*, 61(1):172–182, 2000.
- [32] J. Stoer and R. Bulirsch. *Introduction to Numerical Analysis*, chapter 2, pages 37–144. Springer, New York, 3 edition, 2010.
- [33] William Talbott. Bayesian epistemology. In Edward N. Zalta, editor, *The Stanford Encyclopedia of Philosophy*. Metaphysics Research Lab, Stanford University, winter 2016 edition, 2016.
- [34] J.H. van Lint and R.M. Wilson. The principle of inclusion and exclusion; inversion formulae. In *A Course in Combinatorics*, chapter 10, pages 89–97. Cambridge University Press, Cambridge, 2 edition, 2001.